AMERICAN SOCIETY FOR MICROBIOLOGY | Journal of Bacteriology®

RESEARCH ARTICLE

Conversion of Norepinephrine to 3,4-Dihdroxymandelic Acid in *Escherichia coli* Requires the QseBC Quorum-Sensing System and the FeaR Transcription Factor

Sasikiran Pasupuleti,[a] Nitesh Sule,[a] Michael D. Manson,[b] Arul Jayaraman[a]

[a]Artie McFerrin Department of Chemical Engineering, Texas A&M University, College Station, Texas, USA
[b]Department of Biology, Texas A&M University, College Station, Texas, USA

ABSTRACT The detection of norepinephrine (NE) as a chemoattractant by *Escherichia coli* strain K-12 requires the combined action of the TynA monoamine oxidase and the FeaB aromatic aldehyde dehydrogenase. The role of these enzymes is to convert NE into 3,4-dihydroxymandelic acid (DHMA), which is a potent chemoattractant sensed by the Tsr chemoreceptor. These two enzymes must be induced by prior exposure to NE, and cells that are exposed to NE for the first time initially show minimal chemotaxis toward it. The induction of TynA and FeaB requires the QseC quorum-sensing histidine kinase, and the signaling cascade requires new protein synthesis. Here, we demonstrate that the cognate response regulator for QseC, the transcription factor QseB, is also required for induction. The related quorum-sensing kinase QseE appears not to be part of the signaling pathway, but its cognate response regulator, QseF, which is also a substrate for phosphotransfer from QseC, plays a nonessential role. The promoter of the *feaR* gene, which encodes a transcription factor that has been shown to be essential for the expression of *tynA* and *feaB*, has two predicted QseB-binding sites. One of these sites appears to be in an appropriate position to stimulate transcription from the P_1 promoter of the *feaR* gene. This study unites two well-known pathways: one for expression of genes regulated by catecholamines (QseBC) and one for expression of genes required for metabolism of aromatic amines (FeaR, TynA, and FeaB). This cross talk allows *E. coli* to convert the host-derived and chemotactically inert NE into the potent bacterial chemoattractant DHMA.

IMPORTANCE The chemotaxis of *E. coli* K-12 to norepinephrine (NE) requires the conversion of NE to 3,4-dihydroxymandleic acid (DHMA), and DHMA is both an attractant and inducer of virulence gene expression for a pathogenic enterohemorrhagic *E. coli* (EHEC) strain. The induction of virulence by DHMA and NE requires QseC. The results described here show that the cognate response regulator for QseC, QseB, is also required for conversion of NE into DHMA. Production of DHMA requires induction of a pathway involved in the metabolism of aromatic amines. Thus, the QseBC sensory system provides a direct link between virulence and chemotaxis, suggesting that chemotaxis to host signaling molecules may require that those molecules are first metabolized by bacterial enzymes to generate the actual chemoattractant.

KEYWORDS DHMA, norepinephrine, catecholamines, chemotaxis

Catecholamine hormones and neurotransmitters, an overlapping set of host-derived molecules, profoundly affect the resident microbiota of the mammalian gut (1–3). It is apparent that these molecules are also important in regulating the virulence of invading pathogens (4–7). In particular, the QseBC and QseEF two-

Received 16 September 2017 **Accepted** 3 October 2017

Accepted manuscript posted online 16 October 2017

Citation Pasupuleti S, Sule N, Manson MD, Jayaraman A. 2018. Conversion of norepinephrine to 3,4-dihdroxymandelic acid in *Escherichia coli* requires the QseBC quorum-sensing system and the FeaR transcription factor. J Bacteriol 200:e00564-17. https://doi.org/10.1128/JB.00564-17.

Editor Igor B. Zhulin, University of Tennessee at Knoxville

Address correspondence to Michael D. Manson, mike@mail.bio.tamu.edu, or Arul Jayaraman, arulj@tamu.edu.

component systems of enteric bacteria have been shown to mediate responses to catecholamines (8–14).

We recently demonstrated (15) that some of the effects reported for norepinephrine (NE) and other catecholamines in enterohemorrhagic *Escherichia coli* (EHEC) (16) can also be evoked by a nonamine metabolite of NE, 3,4-dihydroxymandelic acid (DHMA). In addition to inducing virulence gene expression in EHEC, DHMA is a chemoattractant for both EHEC (15) and a nonpathogenic K-12 strain of *E. coli*, RP437 (here referred to as CV1) (17). The chemotaxis response to DHMA is mediated by the Tsr chemoreceptor, which is present in both EHEC and nonpathogenic K-12 strains of *E. coli*. Tsr homologs are present in a number of other enteric bacteria as well, including *Salmonella enterica* (18, 19), *Enterobacter aerogenes* (20), and *Pseudomonas aeruginosa* (21).

DHMA is made from NE in two enzymatic steps. The first step is carried out by a primary amine oxidase, TynA, which produces the intermediate 3,4-dihydroxyphenylglycol-aldehyde (DOPEGAL), and the second step is catalyzed by an aromatic aldehyde dehydrogenase, FeaB (22). TynA and FeaB are also produced by other enteric bacteria, where their characterized function is the utilization of aromatic amines as nitrogen sources and, in at least one case, as a carbon source (23). The expression of TynA and FeaB in *E. coli* CV1 requires prior exposure to NE and subsequent protein synthesis, and the induction of *tynA* and *feaB* transcription depends upon the presence of the histidine protein kinase QseC (17).

FeaR is a transcriptional regulator of the AraC family (23) and has been characterized as an essential transcription factor for the expression of *tynA* and *feaB* in response to exposure to aromatic amines. The *feaR*, *feaB*, and *tynA* genes are adjacent but are divergently transcribed (23). The *feaB* and *tynA* genes have separate promoters and are somewhat differently regulated, although both promoters have two well-defined, tandem FeaR-binding sites upstream of the −35 region of their respective promoters (23).

In this study, we investigated the QseC-dependent signaling pathway by which NE is converted to DHMA. We found that the QseC signaling pathway requires its cognate response regulator QseB and, to a lesser extent, the related response regulator QseF. One output of this pathway is the expression of FeaR. We conclude that cross talk between the regulatory systems for virulence and metabolism of aromatic amines may depend upon the ability of QseBC and, to a lesser extent QseF, to regulate *feaR* as well as genes directly involved in virulence.

RESULTS AND DISCUSSION

The QseC signaling pathway induces TynA and FeaB expression. To study the signaling pathway that induces the enzymes that convert norepinephrine (NE) into the chemoattractant DHMA, we first studied the chemotaxis responses of mutant strains of *E. coli* lacking the relevant sensor kinases (*qseC* or *qseE*) and the corresponding response regulators (*qseB* or *qseF*), using the quantitative motility migration coefficient (MMC) assay (17). All strains responded normally to the control attractant, 10 μM L-serine (Fig. 1). The wild-type strain, CV1, and the CV1Δ*qseE* mutant responded strongly, and essentially identically, to NE in the MMC assay, suggesting that *qseE* is not involved in the conversion of NE to DHMA (Fig. 1). On the other hand, the Δ*qseC* mutant did not respond to NE as an attractant in the MMC assay (Fig. 1), which confirms that QseC plays an essential role. The CV1Δ*qseB* mutant also did not respond to NE, whereas the CV1Δ*qseF* mutant gave a somewhat attenuated chemotaxis response. These results demonstrate that the QseBC histidine kinase/response regulator system is required for induction of TynA and FeaB.

Although the histidine kinase QseE does not seem to play an important role, QseF, the cognate response regulator activated by QseE, does seem to be involved. This observation is consistent with that of Moreira and Sperandio (13), who showed that QseF can also be a substrate for phosphorylation by QseC in *Salmonella*. The MMC values for the CV1, CV1Δ*qseE*, and CV1Δ*qseF* strains were all highest when the NE concentration was 50 μM and were lower at both 5 and 500 μM.

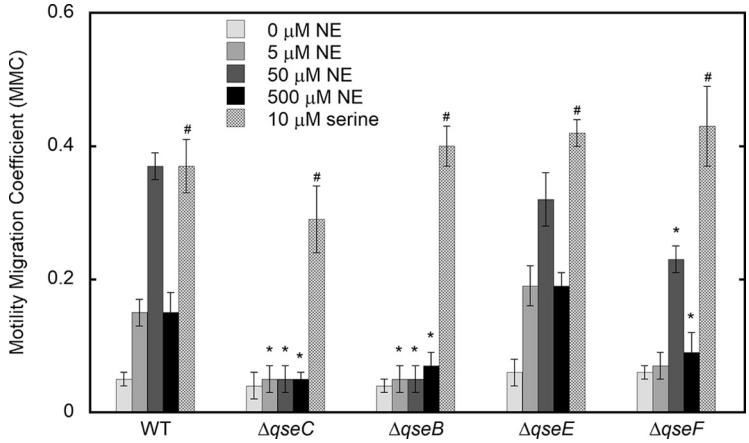

FIG 1 Chemotaxis of *E. coli* CV1 and mutants to NE. Cells were exposed to 0, 5, 50, or 500 μM NE in the microfluidic device, as described in Materials and Methods. Serine (10 μM) was used as the positive control. The motility migration coefficients (MMCs) are shown. Data presented are the means and standard deviations from three independent experiments carried out in duplicate. Statistical significance is shown for the mutant compared to the wild type (WT) at the given NE concentration using the Student *t* test at significance levels of $P < 0.05$ (*). #, statistical significance for serine compared to the buffer control (no NE) in each strain, using the Student *t* test at a significance level of $P < 0.0001$.

It should be noted that the dose-response curve for NE is shifted to higher concentrations by two orders of magnitude compared to that of DHMA (17). This seems to be a reasonable effect, given that NE must be converted to DOPEGAL by TynA in the periplasm, be taken into the cell as DOPEGAL, be converted to DHMA by FeaB, and then exported back to the periplasm to interact with the periplasmic sensory domain of Tsr. We see the same general pattern for the dose response to a step increase in concentration for both DHMA and NE, with a decreased response at higher concentrations as measured in the MMC assay, although shifted to a 100-fold higher concentration with NE.

Role of FeaR in the signaling pathway. The FeaR transcription factor is required for the expression of the *tynA* and *feaB* genes (23, 24). The *feaR*, *tynA*, and *feaB* genes are clustered in the *E. coli* chromosome, with *feaR* being transcribed divergently from the other two. We therefore tested the ability of the CV1Δ*feaR* mutant to respond to NE. These cells responded normally to 10 μM L-serine but failed to respond to NE at any concentration tested (Fig. 2). Thus, FeaR is required for *E. coli* to produce a chemotaxis response to NE, presumably through its role in transcription of the *tynA* and *feaB* genes.

We then determined whether expression of *feaR* increases in cells exposed to NE. Figure 3 shows that *feaR* transcription, as measured by quantitative reverse transcriptase PCR (qRT-PCR), increased by 2.7-fold more when CV1 cells were incubated for 60 min with 8 μM NE than when the cells were incubated for 60 min without NE. No difference in the increase in *feaR* transcription over time, with or without NE incubation, was observed with the CV1Δ*qseC* and CV1Δ*qseB* strains, a result that is consistent with their lack of response in the MMC assay. The increase in the induction of *feaR* transcription in the CV1Δ*qseE* mutant after 60 min of exposure to NE relative to incubation of this strain for 60 min without NE was similar to that seen with CV1 (2.8-fold), indicating that QseE plays little or no role in the signaling pathway. On the other hand, the increase in the transcription of *feaR* in the CV1Δ*qseF* mutant after 60 min exposure to NE was 1.7-fold higher than the increase after 60 min of incubation without NE. This more-modest increase in *feaR* expression suggests that QseF plays some role in the induction of *feaR* transcription. Even in the absence of QseE, phosphorylation of QseF by QseC apparently produces enough QseF-P for full induction of *feaR* transcription.

Induction of TynA and FeaB. Because NE increased the transcription of *feaR*, whose product is known to regulate *tynA* and *feaB*, we next investigated how the transcription

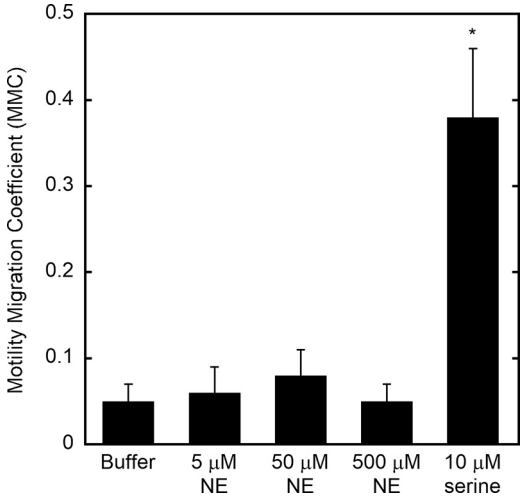

FIG 2 Chemotaxis of *E. coli* CV1 Δ*feaR* to NE. Cells were exposed to 0, 5, 50, and 500 μM NE in the microfluidic device as described in Materials and Methods. Serine (10 μM) was used as the positive control. The motility migration coefficients (MMCs) are shown. Data shown are the means and standard deviations from three independent experiments carried out in duplicate. *, statistical significance for serine compared to the buffer control (no NE), using the Student *t* test at a significance level of $P < 0.0001$.

of *tynA* and *feaB* changes upon incubation with NE in wild-type and mutant strains. Figure 4 shows that the transcription of both *tynA* and *feaB* increased by 2.4-fold more in CV1 cells incubated for 60 min with NE than in cells incubated for 60 min without NE. Consistent with the data in Fig. 3, the increases in transcription of *tynA* and *feaB* in the CV1Δ*qseE* mutant (2.4- and 2.3-fold more, respectively, after 60 min incubation with NE than after 60 min of incubation without NE) were similar to those of the wild type. No difference in the increase in *tynA* or *feaB* transcription with or without NE was seen in the CV1Δ*qseC*, CV1Δ*qseB*, or CV1Δ*feaR* mutants. The CV1Δ*qseF* strain again fell into an intermediate category, with NE boosting transcription of *tynA* and *feaB* 1.7- and 1.6-fold, respectively, after incubation with NE compared to incubation without NE.

Sequence analysis of the *feaR* promoter. An examination of the regulatory region of the *fearR*, *tynA*, and *feaB* genes suggests a mechanism that could explain our results.

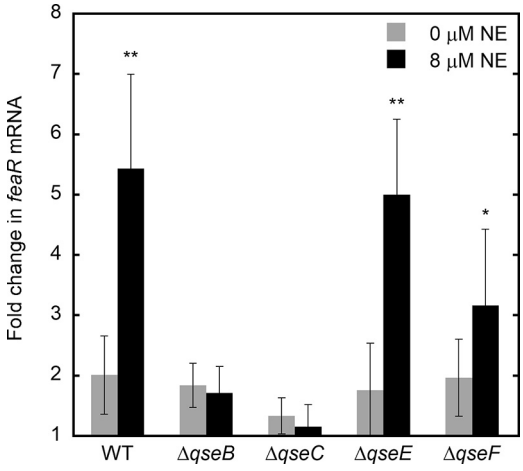

FIG 3 Induction of *feaR* transcription in wild-type (WT) *E. coli* CV1 and the Δ*qse* mutants. The expression of *fea*R was quantified by qRT-PCR before and after incubation for 60 min in cells treated with 8 μM NE. Cells that were incubated without NE for 60 min were used as the negative control. The fold increase in *fea*R mRNA after incubation is shown. Data shown are the means and standard deviations from three independent experiments carried out in duplicate. Statistical significance is shown for NE treatment compared to control, using the Student *t* test at significance levels of $P < 0.05$ (*) and $P < 0.005$ (**).

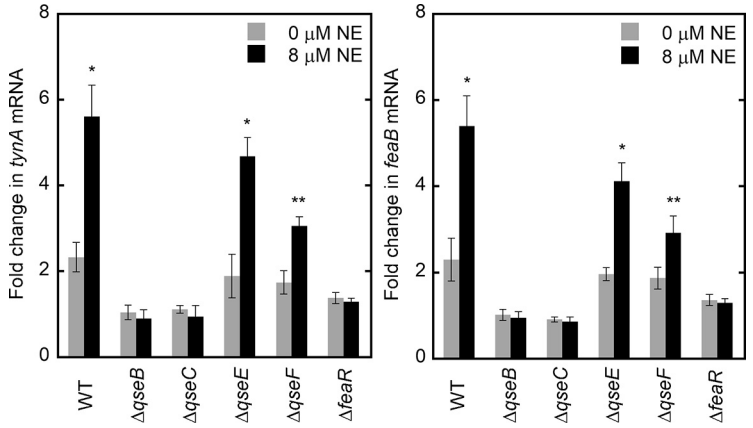

FIG 4 Induction of *tynA* and *feaB* transcription in wild-type (WT) *E. coli* CV1 and Δ*qse* mutants. The expression of *tynA* and *feaB* was quantified by qRT-PCR before and after incubation for 60 min in cells treated with 8 μM NE. Cells that were incubated without NE for 60 min were used as the negative control. The fold increase in *tyn*A (left) and *fea*B (right) mRNA after incubation is shown. Data shown are the means and standard deviations from three independent experiments carried out in duplicate. Statistical significance is shown for NE treatment compared to control, using the Student *t* test at significance levels of $P < 0.05$ (*) and $P < 0.005$ (**).

Both the MMC chemotaxis assay and the analysis of the induction of *feaR*, *feaB*, and *tynA* transcription by pretreatment with NE show that QseC and QseB are essential for production of FeaB and TynA by an indirect mechanism involving the FeaR transcription factor. The data also suggest that the response regulator QseF, which can be phosphorylated both by its cognate histidine kinase QseE and by cross talk from QseC, is required for maximal induction by NE.

Inspection of the *feaR* regulatory region shows that it contains three promoters (23) and two predicted binding sites for QseB (shown in cyan in Fig. 5) (25), based on the consensus binding site of QseB determined for *qseBC* and *flhDC*. One of the QseB-binding sites, which matches the C**AA**TT**A**CGAATT**A** consensus sequence (25) at 9/13 positions and at all four of the highly conserved A bases (in bold and underlined) overlaps the P_m transcription start site, is 11 bp upstream of the −35 region of the P_1 promoter. The other, which matches the consensus at 7/13 positions, at all four of the highly conserved A residues overlaps the P_2 −10 region and transcription start site. Although we do not know which of the three *feaR* promoters is responsible for the induction of *feaR* transcription, the position of the putative QseB-binding sites suggests that the P_1 promoter is the most likely candidate. Also, the P_1 promoter has the closest match to the σ^{70} −35 and −10 consensus sequences.

It is possible that the activity of P_2, and perhaps even transcription initiated at P_1, would be inhibited by the binding of QseB to its downstream binding site. If the affinity

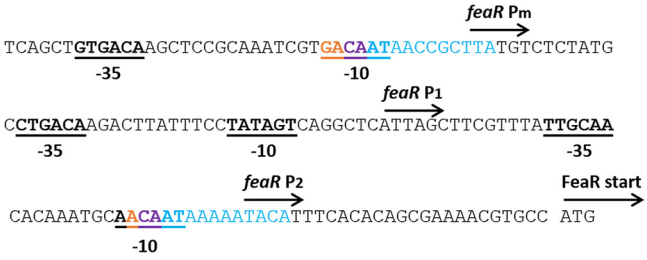

FIG 5 Analysis of the *fea*R promoter. The *feaR* promoter sequence and the predicted QseB-binding sites (32; cyan font) are shown. The last four and three bases (GACA and ACA) of the 3′ ends of the possible QseF binding sites (26) are in orange and, in their two-base overlaps with the 5′ end of the QseB-binding site, in purple type. Proposed promoter elements (−35 and −10) associated with the three mapped transcription start sites are indicated in bold, underlined type, and the transcription start sites are shown by arrows (23).

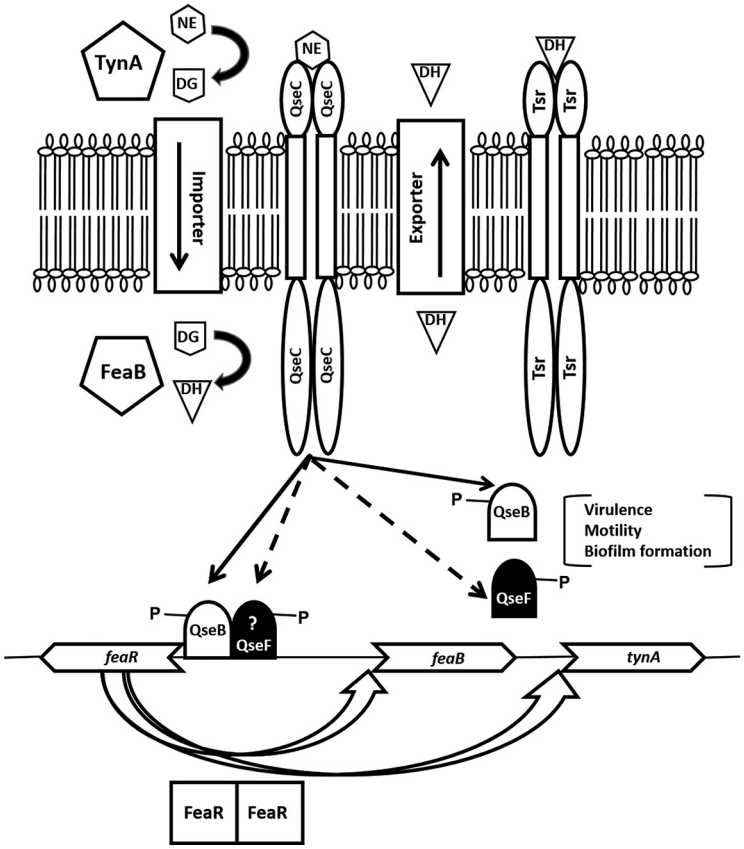

FIG 6 Proposed model for conversion of NE to DHMA. NE binds to QseC, which leads to phosphorylation of QseB and, to a lesser extent, QseF. QseF is also phosphorylated by QseE (not shown) if QseE is present. Phosphorylated QseB (QseB-P), with help from QseF, induces transcription of the *fea*R gene. The FeaR dimer induces the transcription of the *feaB* and *tynA* genes (open arrows) by binding upstream of their respective promoters. Note that QseB-P and QseF-P promote transcription of many genes other than *feaR* (8, 11, 14) and that *feaR* is regulated by numerous transcription factors other than QseB and QseF (23). The TynA protein is exported to the periplasm, where it acts as a monoamine oxidase to convert NE to DOPEGAL (DG). DG is taken by an uncharacterized transporter into the cytoplasm, where the aromatic aldehyde dehydrogenase FeaB oxidizes it to DHMA (DH). DH is delivered by an uncharacterized exporter to the periplasm, where it binds to the Tsr chemoreceptor to evoke an attractant chemotaxis response.

of phosphorylated QseB (QseB-P) for the upstream site is higher than the affinity for the downstream site, *feaR* transcription could be maximally induced at intermediate levels of QseB-P and repressed at higher levels of QseB-P.

The consensus binding site for QseF has been determined for only one gene, *glmY*, which encodes a small noncoding regulatory RNA (26). There is no obvious match to the 18-base QseF consensus sequence in the FeaR regulatory region, although the GACA bases that overlap the −10 region of Pm and the ACA bases that overlap the −35 region of P_2 are the last four and three bases, respectively, of the reported QseF consensus binding site. Although we can make no definitive statement about whether QseF interacts with the *feaR* regulatory region, the short sequence homologies we observe are perhaps in the right position for QseF to bind in conjunction with QseB.

Conclusion. Based on our results, we propose a model to explain how NE induces its own metabolism to DHMA (Fig. 6). In this model, NE binds to QseC to activate its kinase activity. QseC then phosphorylates its cognate response regulator, QseB, and to a lesser extent, the noncognate response regulator, QseF. The phosphorylated response regulators induce transcription of the *feaR* gene, perhaps by binding upstream of the P_1 *feaR* promoter. The FeaR protein, in turn, activates the transcription of the *feaB* and *tynA* genes, whose products convert NE to DHMA. Note that, because of the convoluted way in which NE serves as an attractant, high levels of both TynA and FeaB may be needed to produce enough DHMA to be sensed as an attractant by Tsr.

The paradigm we have just outlined suggests that the extraordinarily thorough work of Julius Adler in the 1960s and 1970s (27) may have missed some important chemoeffectors for *E. coli*, including biological signaling molecules in addition to nutrients For example, we found that the quorum-sensing signal autoinducer-2 is an attractant for *E. coli* that is sensed by binding to the periplasmic LsrB protein, which then interacts with Tsr (28). The realization that a host molecule like NE must be metabolized to DHMA for it to be sensed as an attractant suggests that other important chemoeffectors may be produced only by metabolism. Thus, screens for chemoeffectors should be performed after growing cells in the presence of candidate molecules, a procedure that is routinely followed for organisms like *Pseudomonas putida* that can utilize an enormous catalog of possible organic compounds (29). Such processes for generating chemoeffectors might be important for the pathogenesis of enteric pathogens such as EHEC, as we have observed for NE and DHMA (15). Host-derived compounds like NE and DHMA might also play important roles in interactions among the many organisms of the microbiome.

MATERIALS AND METHODS

Bacterial strains, growth conditions, and materials. *E. coli* RP437 (30), noted here as CV1, was used as the wild-type *E. coli* strain. Green fluorescent protein (GFP)-expressing CV1 cells were obtained by transformation with plasmid pCM18 (31) and used to visualize the response to NE in the microfluidic chemotaxis assay. The pCM18 plasmid was maintained in cultures using 100 μg/ml erythromycin. CV1 *qseB*, *qseE*, *qseF*, or *feaR kan* insertion mutations were generated as described previously (15). Briefly, mutations were introduced into strain CV1 by phage $P1_{vir}$ transduction using lysates generated from the respective mutants in the Keio collection (32). Mutants were selected for kanamycin resistance on lysogeny broth containing 1.2% Difco Bacto agar and 50 μg/ml kanamycin. All gene disruptions were confirmed by PCR.

Liquid cultures were grown in tryptone broth (TB), 10 g/liter tryptone and 8 g/liter NaCl, containing the appropriate antibiotics. Norepinephrine (>99% purity) was obtained from Spectrum Chemicals (Gardena, CA).

Microfluidic chemotaxis assay. Motile bacteria were prepared for chemotaxis assays as described by Mao et al. (33). Cultures of GFP-expressing bacteria were grown in TB containing 100 μg/ml erythromycin. Overnight cultures were inoculated into the same medium to a turbidity at 600 nm of ~0.05. The cultures were grown with swirling in Erlenmeyer flasks at 30°C. At a turbidity of ~0.35, 8 μM NE or solvent blank was added to the cultures and further incubated to mid-exponential phase (turbidity at 600 nm of ~0.5) before being harvested for experiments. Mid-exponential phase cells were centrifuged at 400 × *g* for 10 min at room temperature and gently resuspended in chemotaxis buffer (CB) (physiological buffered saline with 10 mM potassium phosphate, pH 7.0, containing 0.1 mM EDTA, 0.01 mM L-methionine, and 10 mM DL-lactate).

All microflow chemotaxis experiments were performed within 20 min after resuspension of the bacteria in CB. The assay was performed as described previously (15). A mixture of GFP-expressing motile test cells and red fluorescent protein (RFP)-containing dead TG1 cells was gently resuspended in CB. We carefully connected 500-μl gas-tight glass syringes (Hamilton, Reno, NV) containing either CB or CB with chemoeffector to the inlets of the gradient generator module to avoid introducing air bubbles into the device. The bacterial suspension was introduced into the chemotaxis chamber with a 50-μl gas-tight glass syringe. The flow rate in the microfluidic device was maintained at 2.1 μl/min, using a Fusion 400 programmable pump (Chemyx Inc., Stafford, TX). The assembled device was positioned on the stage of a TCS SP5 confocal resonant-scanner microscope (Leica Microsystems Inc., Buffalo Grove, IL). For each assay, 100 images from each fluorophore were collected 7 mm from the inlet at 2.5-s intervals. The 2.5-s imaging interval was chosen based on our calculation that free-floating bacteria moving at a flow rate of 2.1 μl/min take an average of 2.5 s to traverse 1 mm, the imaging field of view (34). The bacteria in the middle of the flow were exposed to the gradient for an average of 18 to 21 s prior to imaging. Cells spending more time in contact with the floor or ceiling of the chamber move more slowly (34).

Quantification of chemotaxis in the microflow assay with image analysis. The migration and distribution of bacteria in each image were quantified using a program developed in-house. Briefly, the analysis consisted of the following steps: (i) removal of background pixels in the image, based on pixel size and intensities; (ii) determination of the center of the flow chamber (i.e., where bacteria enter the observation chamber), using dead cells (red fluorescence) as a reference; (iii) location of green cells (i.e., live bacteria expressing GFP) in the images relative to the center, by determining the centroid; and (iv) calculation of the MMC based on the location of the migrated motile cells. These steps were repeated for each image, and the total counts of cells in 100 images were summed for analysis to generate migration profiles. The MMC is calculated by weighting the migration of cells by the distance they move in either direction from the center of the observation chamber, as previously described (15). The MMC value represents the extent of the smooth-swimming response of cells in CB that are introduced into a chamber with a uniform concentration of attractant. The cells do not adapt to the attractant until they spread across the chamber. If they adapt before reaching the point along the channel at which their

distribution is imaged, their movement is random run-and-tumble behavior that will not significantly affect the final distribution across the chamber.

RNA isolation and qRT-PCR. Bacteria were grown in TB as described above, and the mutant strains were grown in the presence of 50 μg/ml kanamycin. At mid-exponential phase (after 60 min of exposure to NE), cell pellets were collected by centrifugation and stored in RNAprotect reagent (Qiagen, CA) at −80°C prior to RNA extraction. Total RNA was isolated from the cell pellet using an RNeasy minikit (Qiagen, CA) with the protocol provided by the manufacturer. RNA purity was assessed using the ratio of absorbance 260/280 nm. All samples had an A_{260}/A_{280} ratio of >2.0. qRT-PCR was performed on a LightCycler 96 (Roche, IN) using an iScript one-step reverse transcriptase PCR (RT-PCR) kit with SYBR green (Bio-Rad Laboratories, CA) and gene-specific primers using the protocol recommended by the manufacturer. The reaction volume was 25 μl, with 50 ng of RNA per reaction and 0.15 μM each primer. The threshold cycle numbers (C_T), were obtained using the LightCycler system software (Roche, CA). Fold-changes in expression with NE exposure relative to untreated cells were calculated using the $\Delta\Delta C_T$ method (35), and the *rrsG* (rRNA G) transcript was used as the housekeeping gene for data normalization. All qRT-PCR experiments were repeated with three different cultures and two technical replicates per culture.

ACKNOWLEDGMENTS

This work was supported in part by the Nesbitt Chair endowment to A.J. and by the National Science Foundation (grant MCB 1121916) to M.D.M. and A.J.

REFERENCES

1. Lyte M, Vulchanova L, Brown DR. 2011. Stress at the intestinal surface: catecholamines and mucosa–bacteria interactions. Cell Tissue Res 343:23–32. https://doi.org/10.1007/s00441-010-1050-0. 20941511.
2. Freestone P. 2013. Communication between bacteria and their hosts. Scientifica (Cairo) 2013:361073. https://doi.org/10.1155/2013/361073.
3. Stevens MP. 2010. Modulation of the interaction of enteric bacteria with intestinal mucosa by stress-related catecholamines, p 111–134. *In* Lyte M, Freestone PPE (ed), Microbial endocrinology. Springer, New York, NY.
4. Bansal T, Englert D, Lee J, Hegde M, Wood TK, Jayaraman A. 2007. Differential effects of epinephrine, norepinephrine, and indole on *Escherichia coli* O157: H7 chemotaxis, colonization, and gene expression. Infect Immun 75:4597–4607. https://doi.org/10.1128/IAI.00630-07.
5. Lyte M, Arulanandam BP, Frank CD. 1996. Production of Shiga-like toxins by *Escherichia coli* O157: H7 can be influenced by the neuroendocrine hormone norepinephrine. J Lab Clin Med 128:392–398. https://doi.org/10.1016/S0022-2143(96)80011-4.
6. Lyte M, Erickson AK, Arulanandam BP, Frank CD, Crawford MA, Francis DH. 1997. Norepinephrine-induced expression of the K99 pilus adhesin of enterotoxigenic *Escherichia coli*. Biochem Biophys Res Commun 232:682–686. https://doi.org/10.1006/bbrc.1997.6356.
7. Lyte M, Freestone PP, Neal CP, Olson BA, Haigh RD, Bayston R, Williams PH. 2003. Stimulation of *Staphylococcus epidermidis* growth and biofilm formation by catecholamine inotropes. Lancet 361:130–135. https://doi.org/10.1016/S0140-6736(03)12231-3.
8. Sperandio V, Torres AG, Kaper JB. 2002. Quorum sensing *Escherichia coli* regulators B and C (QseBC): a novel two-component regulatory system involved in the regulation of flagella and motility by quorum sensing in *E. coli*. Mol Microbiol 43:809–821. https://doi.org/10.1046/j.1365-2958.2002.02803.x.
9. Clarke MB, Hughes DT, Zhu C, Boedeker EC, Sperandio V. 2006. The QseC sensor kinase: a bacterial adrenergic receptor. Proc Natl Acad Sci U S A 103:10420–10425. https://doi.org/10.1073/pnas.0604343103.
10. Reading NC, Torres AG, Kendall MM, Hughes DT, Yamamoto K, Sperandio V. 2007. A novel two-component signaling system that activates transcription of an enterohemorrhagic *Escherichia coli* effector involved in remodeling of host actin. J Bacteriol 189:2468–2476. https://doi.org/10.1128/JB.01848-06.
11. Hughes DT, Clarke MB, Yamamoto K, Rasko DA, Sperandio V. 2009. The QseC adrenergic signaling cascade in enterohemorrhagic *E. coli* (EHEC). PLoS Pathog 5:e1000553. https://doi.org/10.1371/journal.ppat.1000553.
12. Moreira CG, Weinshenker D, Sperandio V. 2010. QseC mediates *Salmonella enterica* serovar Typhimurium virulence *in vitro* and *in vivo*. Infect Immun 78:914–926. https://doi.org/10.1128/IAI.01038-09.
13. Moreira CG, Sperandio V. 2012. Interplay between the QseC and QseE bacterial adrenergic sensor kinases in *Salmonella enterica* serovar Typhimurium pathogenesis. Infect Immun 80:4344–4353. https://doi.org/10.1128/IAI.00803-12.
14. Weigel W, Demuth D. 2016. QseBC, a two-component bacterial adrenergic receptor and global regulator of virulence in *Enterobacteriaceae* and *Pasteurellaceae*. Mol Oral Microbiol 31:379–397. https://doi.org/10.1111/omi.12138.
15. Sule N, Pasupuleti S, Kohli N, Menon R, Dangott LJ, Manson MD, Jayaraman A. 2017. The norepinephrine metabolite 3,4-dihydroxymandelic acid is produced by the commensal microbiota and promotes chemotaxis and virulence gene expression in enterohemorrhagic *Escherichia coli*. Infect Immun 85:e00431-17. https://doi.org/10.1128/IAI.00431-17.
16. Walters M, Sperandio V. 2006. Autoinducer 3 and epinephrine signaling in the kinetics of locus of enterocyte effacement gene expression in enterohemorrhagic *Escherichia coli*. Infect Immun 74:5445–5455. https://doi.org/10.1128/IAI.00099-06.
17. Pasupuleti S, Sule N, Cohn WB, MacKenzie DS, Jayaraman A, Manson MD. 2014. Chemotaxis of *Escherichia coli* to norepinephrine (NE) requires conversion of NE to 3,4-dihydroxymandelic acid. J Bacteriol 196:3992–4000. https://doi.org/10.1128/JB.02065-14.
18. Iwama T, Nakao K-I, Nakazato H, Yamagata S, Homma M, Kawagishi I. 2000. Mutational analysis of ligand recognition by Tcp, the citrate chemoreceptor of serovar Typhimurium. J Bacteriol 182:1437–1441. https://doi.org/10.1128/JB.182.5.1437-1441.2000.
19. Wang Q, Mariconda S, Suzuki A, McClelland M, Harshey RM. 2006. Uncovering a large set of genes that affect surface motility in *Salmonella enterica* serovar Typhimurium. J Bacteriol 188:7981–7984. https://doi.org/10.1128/JB.00852-06.
20. Dahl MK, Boos W, Manson MD. 1989. Evolution of chemotactic-signal transducers in enteric bacteria. J Bacteriol 171:2361–2371. https://doi.org/10.1128/jb.171.5.2361-2371.1989.
21. Craven RC, Montie TC. 1983. Chemotaxis of *Pseudomonas aeruginosa*: involvement of methylation. J Bacteriol 154:780–786.
22. Rankin LD, Bodenmiller DM, Partridge JD, Nishino SF, Spain JC, Spiro S. 2008. *Escherichia coli* NsrR regulates a pathway for the oxidation of 3-nitrotyramine to 4-hydroxy-3-nitrophenylacetate. J Bacteriol 190:6170–6177. https://doi.org/10.1128/JB.00508-08.
23. Zeng J, Spiro S. 2013. Finely tuned regulation of the aromatic amine degradation pathway in *Escherichia coli*. J Bacteriol 195:5141–5150. https://doi.org/10.1128/JB.00837-13.
24. Hanlon SP, Hill TK, Flavell MA, Stringfellow JM, Cooper RA. 1997. 2-phenylethylamine catabolism by *Escherichia coli* K-12: gene organization and expression. Microbiology 143:513–518. https://doi.org/10.1099/00221287-143-2-513.
25. Clarke MB, Sperandio V. 2005. Transcriptional regulation of *flhDC* by QseBC and σ^{28} (FliA) in enterohaemorrhagic *Escherichia coli*. Molec Microbiol 57:1734–1749. https://doi.org/10.1111/j.1365-2958.2005.04792.x.
26. Gopel Y, Luttmann D, Heroven AK, Reichenbach B, Dersch P, Gorke B. 2011. Common and divergent features in transcriptional control of the homologous small RNAs GlmY and GlmZ in *Enterobacteriaceae*. Nucleic Acids Res 39:1294–1309. https://doi.org/10.1093/nar/gkq986.

27. Kresge N, Simoni RD, Hill RL. 2006. Julius Adler's contributions to understanding bacterial chemotaxis. J Biol Chem 281:e33.
28. Hegde M, Englert DL, Schrock S, Cohn WB, Vogt C, Wood TK, Manson MD, Jayaraman A. 2011. Chemotaxis to the quorum-sensing signal AI-2 requires the Tsr chemoreceptor and the periplasmic LsrB AI-2-binding protein. J Bacteriol 193:768–773. https://doi.org/10.1128/JB.01196-10.
29. Parales RE, Luu RA, Hughes JG, Ditty JL. 2015. Bacterial chemotaxis to xenobiotic chemicals and naturally occurring analogs. Curr Opin Biotechnol 33:318–326. https://doi.org/10.1016/j.copbio.2015.03.017.
30. Parkinson JS, Houts SE. 1982. Isolation and behavior of *Escherichia coli* deletion mutants lacking chemotaxis functions. J Bacteriol 151:106–113.
31. Hansen MC, Palmer RJ, Jr, Udsen C, White DC, Molin S. 2001. Assessment of GFP fluorescence in cells of *Streptococcus gordonii* under conditions of low pH and low oxygen concentration. Microbiology 147:1383–1391. https://doi.org/10.1099/00221287-147-5-1383.
32. Baba T, Ara T, Hasegawa T, Takai Y, Okumura Y, Baba M, Datsenko KA, Tomita M, Wanner BL, Mori H. 2006. Construction of *Escherichia coli* K-12 in-frame, single-gene knockout mutants: the Keio collection. Mol Syst Biol 2:2006.0008. https://doi.org/10.1038/msb4100050.
33. Mao H, Kremer PS, Manson MD. 2003. A senstive, versatile microfluidic assay for bacterial chemotaxis. Proc Natl Acad Sci U S A 100:5449–5454. https://doi.org/10.1073/pnas.0931258100.
34. Englert DL, Manson MD, Jayaraman A. 2009. Flow-based microfluidic device for quantifying bacterial chemotaxis in stable, competing gradients. Appl Environ Microbiol 75:4557–4564. https://doi.org/10.1128/AEM.02952-08.
35. Rao X, Huang X, Zhou Z, Lin X. 2013. An improvement of the 2^ (-delta delta CT) method for quantitative real-time polymerase chain reaction data analysis. Biostat Bioinforma Biomath 3:71–85.